Biophysical Chemistry, 31 (1988) 247–258
Elsevier



BPC 01273

# Study of the translational diffusion of macromolecules in beads of gel chromatography by the FRAP method

Eric Poitevin and Philippe Wahl

*Centre de Biophysique Moléculaire, C.N.R.S., 1A, Avenue de la Recherche Scientifique, 45071 Orléans Cedex 2, France*

Received 1 February 1988
Revised manuscript received 29 April 1988
Accepted 2 May 1988

Translational diffusion; Fluorescein isothiocyanate dextran; Sephadex gel; Partition coefficient; Size-exclusion chromatography

We measured the translational diffusion of fractions of dextrans labelled with fluorescein isothiocyanate, in Sephadex gel beads permeated by aqueous solutions of these molecules. The molecular weights of these fractions were between 5400 and 200000 and measurements of their diffusion coefficients inside a gel bead ($D$) and in the free solution ($D_0$), were performed using the fluorescence recovery after photobleaching method (FRAP). We also determined the coefficient of partitioning ($K_{av}$) of these fractions between the gel and the free solvent, with a new microfluorimetric method. We found that, for Sephadex G-50, G-75, G-100, G-150 and G-200 gels, $K_{av}$ varied with the Stokes radius ($r_s$) of the dextran molecules, in agreement with the formula of Laurent and Killander (J. Chromatogr. 14 (1964) 317). For Sephadex G-100, G-150 and G-200 gels, $D/D_0$ varied with $r_s$, according to the theory of Ogston et al. (Proc. R. Soc. Lond. 333 (1973) 297). In addition, these theories predict a relation linking $D/D_0$ to $K_{av}$ which was well verified. Our work is the first systematic study of the translational diffusion of macromolecules in a chromatography gel. These measurements should allow a better evaluation of the factors which influence the resolution in exclusion chromatography. In addition, the diffusion of macromolecules in gels may provide models for the diffusion of these molecules in the cytoplasm of living cells and in connective biological tissues.

## 1. Introduction

The principle of separation of chemical compounds by liquid chromatography is based on the differential partitioning of their molecules between a fluid and a stationary phase. In exclusion chromatography, the stationary phase is constituted by gel beads packed in a column. The matrix of the gel is a polymer cross-linked by stable chemical bonds. The porous structure of the gel behaves as a molecular sieve which separates the molecules according to their size [1–3].

The rate of progress of permeation of the solute into the gel beads is one of the main factors which determine the efficiency of a chromatography medium. This means that the height of the equivalent theoretical plate (HETP) which characterizes the chromatography resolution depends strongly on the translational diffusion coefficients of the solutes in the gel [4,5].

Until now, very few works dealing with measurements of solute diffusion in gels have been published. This situation probably results from the difficulties encountered in applying the usual methods of diffusion measurements in free solution to gels. Ackers and Steere [6], however, determined the diffusion of proteins in an agarose gel by measuring the rate of transfer of solute molecules between two compartments separated by a thin agarose gel membrane [6]; Davis [7] studied the diffusion of proteins labelled with $^{125}I$ in polyacrylamide blocks. More recently, the diffusion of commercial dextran samples and of two

Correspondence address: P. Wahl, Centre de Biophysique Moléculaire, C.N.R.S., 45071 Orléans Cedex 2, France.

proteins was studied in alginate and in agarose gels through measurements of the spectral broadening of the scattering light [8,40].

In order to avoid the difficulties presented by studies of diffusion in gels, Laurent and Pietruszkiewitz [9] and Laurent et al. [10] measured the diffusion and sedimentation of various compact particles in hyaluronic acid solutions. These authors estimated that the hyaluronic acid formed a three-dimensional network in these solutions, which slowed down the motion of the compact particles, giving rise to what they called a 'sieve effect'. These sedimentation data were fitted by the following formula:

$$s/s_0 = A \exp[-BC^{\nu}] \quad (1)$$

where $s$ and $s_0$ are the sedimentation coefficients of the solute in the hyaluronic acid solution and in the free solvent, respectively, $\nu$ is equal to 0.5, $C$ the hyaluronic acid concentration, and $A$ and $B$ constants depending on the particle radius. $B$ is proportional to this radius. A similar effect on the sedimentation of two globular proteins in various aqueous polymer solutions was observed by Laurent and Persson [11].

A theoretical explanation of the empirical equation (eq. 1) was provided by Ogston et al. [12] who showed that a similar relation could also be applied to diffusion of the particles in polymer solutions. The theory considered the effect of fixed barriers on migration of the solute. These barriers were formed by a random distribution of long molecular fibers, a model previously introduced by Ogston [13] and Laurent and Killander [14] in a theoretical derivation of the partition coefficient $K_{av}$ which determined the elution volume in gel exclusion chromatography.

More recently, Langevin and Rondelez [15] studied the sedimentation of bovine serum albumin and of compact viruses in semidilute aqueous solutions of polyethylene oxide. According to theory, polymer molecules are entangled in semidilute polymer solutions. It is possible to define a correlation length which characterizes the average distance between the entanglement points [16,17]. The ratio of the friction coefficients of a particle in the free solvent and in the polymer solution follows a scaling law [18].

In fact, eq. 1 can be considered as an example of the scaling law. Langevin and Rondelez found that this formula could represent their results with $\nu = 0.62$.

Other authors measured the diffusion of small spheres of polystyrene latex in various semidilute polymer solutions, using the quasi-elastic scattering method. The diffusion of spheres of 100 nm diameter in polyxanthine solutions obeyed the formula of Ogston et al., as observed in ref. 19. On the other hand, the diffusion properties of spheres of various diameters suspended in polyacrylic acid of different molecular mass or in dextran solutions could not be explained by a scaling law [20].

In a recent work, Cukier [21] calculated the diffusion coefficient of spherical particles in semidilute solutions of rod-shaped or flexible macromolecules. The final formula derived by this author, expressing $D/D_0$ as a function of the concentration of macromolecule and of particle radius, was similar to that of Ogston et al. [12].

The brief discussion above shows that there is no theory explaining all the experimental determinations of the transport properties of particles in semidilute polymer solutions. In addition, these solutions do not necessarily present the same properties as the cross-linked gels, since the entanglement points are labile in polymer solutions and fixed in gels.

It has been suggested that the diffusion of macromolecules in gels constitutes a simple model for the diffusion of these molecules in cytoplasm where protein fibers form a three-dimensional matrix [22].

The fluorescence recovery after photobleaching (FRAP) technique allows one to measure the diffusion coefficient $D$ of dextran labelled with fluorescein isothiocyanate injected into the cytoplasm of living cells, and to show that this diffusion coefficient is smaller than that $D_0$ of the same molecules in a free aqueous solvent. The ratio $D/D_0$ decreases with the size of the dextran molecules, which shows that the cytoplasmic matrix exerts a 'sieve effect' on diffusion of dextran [23]. The study of this diffusion provides information on the structure of the cytoplasmic matrix [23,24].

The discussion developed in this section shows that translational diffusion measurements of mac-

romolecule solutions included in gel matrices and especially in chromatographic gel beads should be very useful. In addition, FRAP appears to be a technique that is well-suited for such measurements [22].

In the present work, we measured the diffusion of dextran-FITC of various molecular masses in single beads of Sephadex G-25, G-50, G-75, G-100, G-150 and G-200. These gels are composed of dextrans and differ from one another in degree of reticulation [25]. They were the first exclusion chromatography gels to become commercially available and have been used extensively in order to separate proteins and dextrans.

Our dextran-FITCs were also commercial samples which we fractionated by chromatography on a Sephadex G-200 gel column. We measured the diffusion coefficient of a number of fractions in aqueous solutions by the FRAP method and calculated their Stokes radius. We determined dextran partitioning between a single Sephadex gel bead and the surrounding free solvent by a new microfluorimetric method in which the fluorescence was excited by a focussed laser beam, the direction of which was perpendicular to the optical axis of the microscope which collected the fluorescence. With the same optical arrangement, we determined the ratio $D/D_0$ by the FRAP method. For the Sephadex G-200, G-150 and G-100 gels, our results were in fair agreement with the expression of Laurent and Killander [14] on the one hand and with that of Ogston et al. [12], on the other.

## 2. Materials and methods

Dextrans labelled with fluorescein isothiocyanate (dextran-FITCs) were purchased from Sigma (St. Louis, U.S.A.). Their respective commercial name, lot no., average molecular mass (in Da) and degree of substitution (in mol FITC per mol glucose) were: FD-4 (74 F- 0326, 4100, 0.003), FD-10S (24 F- 5009, 9000, 0.01), FD-20S (80 F-8120, 17500, 0.008), FD-40S (80 F- 8060, 41000, 0.0082), FD-70S (71 F- 5024, 64200, 0.01), FD-150 (122 F- 0948, 156900, 0.004).

Sephadex gels were obtained from Pharmacia-France. Their commercial designations and lot nos. were G-200 (lot no. 6471), G-150 (5742), G-100 (5484), G-75 (GH 21970), G-50 coarse (GG 19324) and G-25 coarse (8219).

The concentrations of Sephadex gel matrices were determined from the following equation [1,26]:

$$C = d/(1 + S_r d) \quad (2)$$

where $d = 1.64$ g/cm$^3$ is the density of dextran, and $S_r$ the water regain, i.e., the volume of water per unit mass of dextran, provided by the manufacturer.

### 2.1. Fractionation of dextran-FITC samples by Sephadex gel chromatography

The six commercial dextran-FITC samples were dissolved in 4 ml of 0.01 M phosphate buffer (pH 7.1), 0.1 M NaCl at concentrations between 0.1 and 0.6 mg/ml. 2 ml of these solutions were injected into a Sephadex gel column (1.61 × 88.5 cm$^3$) eluted with the same buffer at a flow rate of 7 cm h$^{-1}$. Fractions of 2.5 ml were collected at the bottom of the column. We only kept for this work those fractions having an elution volume close to that of the elution profile maximum.

A second chromatographic run with the FD-20S sample was performed on a similar column. The volume and concentration of the injected solution were 1.5 ml and 6 mg/ml, respectively, and the volumes of collected fractions were 1.8 ml. All fractions were stored at −20 °C.

The relative concentration of dextrans in fractions was obtained by fluorescence intensity measurements with a JY3C spectrofluorimeter (Jobin-Yvon, France). The excitation wavelengths were 493 or 420 nm, in order to avoid the optical screening effect. The emission wavelength was 510 nm. Calibration of the fluorescence intensity with crude dextran-FITC samples of known concentration allowed us to determine the concentration of dextran-FITC in the chromatography fractions.

The chromatographic partition coefficients of the fractions were computed according to Laurent and Killander [14] by the following expression:

$$K_{av} = \frac{V_e - V_0}{V_T - V_0} \quad (2)$$

where $V_e$ is the fraction elution volume, $V_T$ the column volume and $V_0$ the void volume obtained by passing Blue Dextran 2000 (Pharmacia lot 6 B19049) through the column.

### 2.2. Apparatus for measuring the diffusion and partition coefficients

The apparatus which was used for FRAP and microfluorimetric measurements has already been described [27,28]. It is similar to published FRAP apparatuses [29] (fig. 1).

The bleaching and monitoring beams were obtained by passing the 488 nm radiation from an argon ion laser (Spectraphysics 164) through a modulating device of the Mach-Zehnder interferometer type. The sample was placed on the stage of a Zeiss universal microscope equipped with a III RS vertical illuminator. The beam of the sample fluorescence collected by the microscope objective passed through a barrier filter (LP 520), the measuring diaphragm of the Zeiss 01 K photometer, and impinged on the photocathode of a 56 TVP photomultiplier (Radiotechnique) cooled at $-20\,^{\circ}C$. The fluorescence intensity was measured by photoelectron pulse counting on a 100 MHZ Canberra 2071 A counter which was interfaced with a Minc 23 computer.

### 2.3. Determination of the absolute coefficient of diffusion and the Stokes radius

For these measurements, the laser beam was directed on the dichroic mirror of the vertical illuminator and focussed on the center of the microscope object plane by an objective of power 4 and NA 0.1 (fig. 1). The beam diameters was 48.3 or 64.8 $\mu$m in the object plane.

The sample was introduced in a microslide of 200 $\mu$m optical path (Camlab, Cambridge, U.K.), with its middle plane set in the microscope object plane.

The diffusion coefficient of a fluorescent sample was obtained from the value of the half-time of the fluorescence recovery time $t_{1/2}$, according to the following formula [30,31]:

$$D_0 = \frac{\beta W^2}{4t_{1/2}} \quad (3)$$

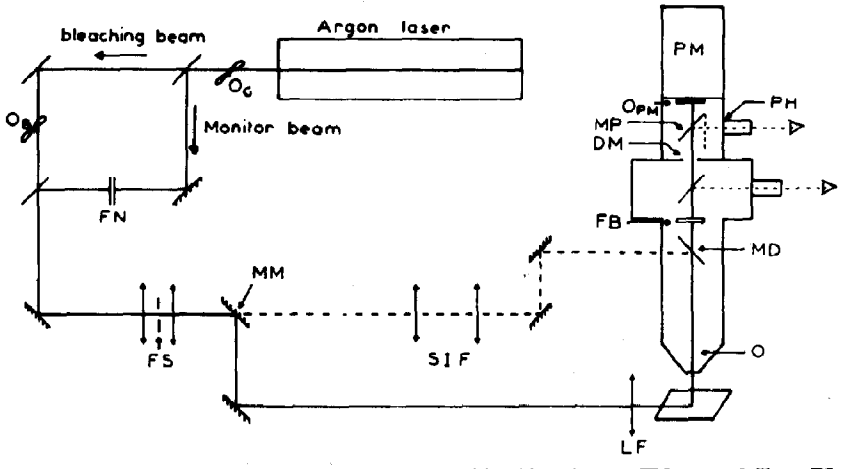


Fig. 1. Optical arrangement in the FRAP apparatus. OG, shutter; OB, bleaching shutter; FN, neutral filter; FS, spatial filter; MD, dichroic mirror; O, microscope objective; FB, barrier filter; DM, measuring diaphragm; MP, swivelling mirror; OPM, photomultiplier shutter; PM, photomultiplier; PH, photometer; vertical illumination was obtained when the mirror (MM) was removed; SIF, intermediary focussing system; LF, focussing lens.

where $W$ is the radius of the laser beam in the microscope object plane, and $\beta$ a factor which depends on the bleached fraction [30]; $t_{1/2}$ was obtained either graphically [31] or by a least-squares fit of the linearized FRAP curve [30].

From the FRAP curve, one could also determine the fraction of freely diffusing molecules defined by the following formula:

$$L = (F_\infty - F_0)/(F_i - F_0) \quad (4)$$

where $F_i$, $F_0$ and $F_\infty$ are the fluorescence intensities before bleaching, immediately after the bleaching light pulse, and at infinite time, respectively.

The Stokes radius $r_s$ is related to $D_0$ by the Stokes-Einstein formula [32]:

$$D_0 = \frac{kT}{6\pi\eta r_s} \quad (5)$$

where $k$, $T$ and $\eta$ are Boltzmann's constant, the absolute temperature and the solvent viscosity, respectively.

### 2.4. Microfluorimetric measurements of the partition coefficient

These measurements were performed with the instrument described above. In this case, however, the laser beams, after being reflected on adjustable mirrors, were projected by a lens of 100 mm focal length into the microscope object plane and crossed the optical microscope axis at right angles (fig. 1). The beam radius in the center of the microscope optical field was about 20 $\mu$m. The fluorescence was collected by the microscope equipped with a Neofluar objective of power 10 and NA 0.35. The bleaching shutter was permanently closed.

A solution of fluorescent dextran containing a few gel beads was introduced into a quartz spectrofluorimeter cell of square cross-section, and four transparent sides. The optical path in the cell was 3 mm. The cell, closed by a tight teflon stopper, was laid horizontally on a special holder, and placed on the microscope stage with two of its transparent sides perpendicular to the microscopic axis, the two other sides being perpendicular to the laser beam (fig. 2). The gel beads fell down to the lower optical side of the cuvette. One of these beads, of diameter between 140 and 300 $\mu$m, was centered in the optical field of the microscope, its middle plane brought into focus. Under these conditions, the laser beam went into the bead through its longest diameter in the microscope's focal plane. This was achieved by careful adjustments of the mirrors and of the focussing lens, and checked by observing the fluorescence trace of the laser in the bead and the surrounding free solvent.

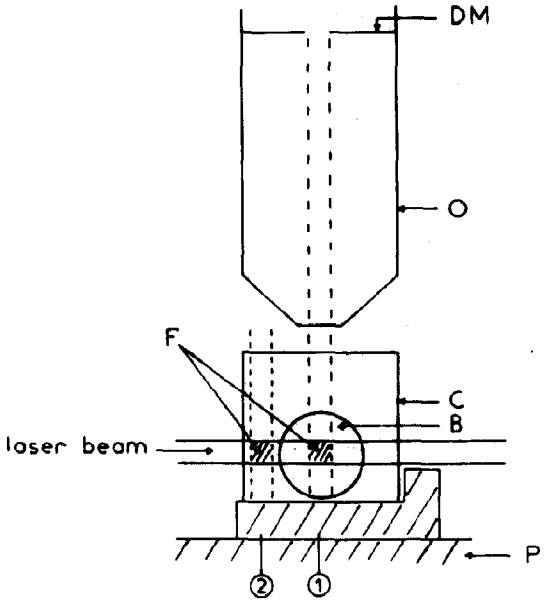


Fig. 2. Experimental arrangement of the laser beam and of the sample used for measurements of the partition coefficient and of the ratio $D/D_0$. DM, measuring diaphragm; O, microscope objective; C, sample cell; B, gel bead; F, sample volume, the fluorescence of which was measured; P, microscope stage. Points 1 and 2 of the microscope stage were centered on the optical axis of the microscope when the fluorescence was measured inside and outside the gel bead, respectively.

The measuring diaphragm of the microscope photometer delimited a segment of the fluorescence trace of the laser beam, of length 35 $\mu$m, in the center of the gel bead.

Let $F_B$ be the photoelectric pulse counts measured under these conditions. By means of a small

horizontal displacement of the stage perpendicularly to the direction of the laser beam, we measured the photocounts $F_I$ of the segment of the fluorescence beam trace in the surrounding free solution. We could then write:

$$\frac{F_B}{F_I} = \frac{C_B Q_B V_B}{C_I Q_I V_I} \tag{6}$$

where $C_B$, $Q_B$, $V_B$, $C_I$, $Q_I$ and $V_I$ are the solute concentrations, fluorescence quantum yields and measured volumes in the bead and in the free solvent, respectively. Since the difference in refractive index between the two media was small, one could consider that $V_B = V_I$. Assuming further that $Q_B = Q_I$, one obtains from [6]:

$$\frac{F_B}{F_I} = \frac{C_B}{C_I} = K_{av} \tag{7}$$

Eqs. 6 and 7 were valid when the fluorescent chromophore concentration was low enough to avoid the filter effect due to laser beam absorption in the solution. It was also necessary to ensure that no other bead intercepted the laser beam in front of the bead chosen for measurement. The sensitivity and accuracy of this fluorimetric method were limited by stray light, which set the smallest measurable $K_{av}$ value equal to 0.02. This performance could probably be improved if a smaller sample cuvette is used.

With this microfluorimetric technique, we were able to measure differences in $K_{av}$ between beads belonging to the same commercial lot. One could also detect inhomogeneities in the solute distribution inside a bead.

### 2.5. Determination of the ratio of diffusion coefficients of dextran molecules inside and outside a Sephadex bead

By actuating the shutter which stopped the bleaching laser beam, we could record two FRAP curves successively with the optical set-up used for determination of $K_{av}$. One FRAP curve was measured with a bead centered on the microscope's optical field, the other being taken from the surrounding solution. The ratio of the diffusion coefficients $D$ and $D_0$ was obtained from the following expression:

$$\frac{D}{D_0} = \frac{\beta}{\beta_0} \frac{t_{01/2}}{t_{1/2}} \tag{8}$$

where $\beta_0$, $t_{01/2}$ and $\beta$, $t_{1/2}$ are relative to the free solution and the solution included in the bead, respectively.

### 2.6. The theory of Laurent and Killander for partitioning between a gel and the free solvent

Laurent and Killander [14] expressed the coefficient of partioning of macromolecules in a gel as follows:

$$K_{av} = \exp\left[-(r_s + r_f)^2 \pi l\right] \tag{9}$$

where $r_s$, $r_f$ and $l$ are the Stokes radius of the solute molecules, the cross-sectional radius of the gel fibers and the linear concentration of these fibers in the gel, respectively.

In order to obtain this expression, $K_{av}$ was assumed to be equal to the probability that a spherical particle was included in a network of fibers of infinite length, a probability which had previously been computed by Ogston [13]. $l$ is related to the mass concentration $C$ of the gel fibers by the relation:

$$r_f^2 l = C\bar{v} \tag{10}$$

where $\bar{v}$ is the partial specific volume of the fibers.

Eq. 9 can also be written:

$$(-\ln K_{av})^{1/2} = (r_s + r_f)(\pi l)^{1/2} \tag{11}$$

The average pore radius of gel cavities can be defined as follows [13]:

$$\rho = (4l)^{-1/2} - r_f \tag{12}$$

### 2.7. Diffusion of solute molecules in a gel: theory of Ogston et al. [12]

In order to explain the empirical equation which was proposed by Laurent et al. [10] to describe their sedimentation measurements of compact

particles in solutions of hyaluronic acid, Ogston et al. [12] elaborated a theory on the transport properties of spherical particles in a solution of infinite, straight fibers which constituted the gel model in the previous calculation of Ogston [13] mentioned above.

Ogston et al. [12] considered the fibers as barriers which reduced the root mean square unit displacement of the solute particles, and derived the following formula from their calculations:

$$\frac{D}{D_0} = \exp\left[-(r_s + r_f)(\pi l)^{1/2}\right] \tag{13}$$

where $D$ and $D_0$ are the particle diffusion coefficient in the fiber solution and in the pure solvent, respectively. Eq. 13 can also be written:

$$-\ln\left(\frac{D}{D_0}\right) = (r_s + r_f)(\pi l)^{1/2} \tag{14}$$

From eqs. 11 and 14, we can immediately write [12]:

$$(-\ln K_{av})^{1/2} = -\ln\left(\frac{D}{D_0}\right) \tag{15}$$

## 3. Results

### 3.1. Fractionation of crude dextran-FITC samples

The six commercial samples of dextran-FITC were chromatographed on a Sephadex G-200 column under the conditions described in section 2. The FD-20S sample was chromatographed a second time under slightly different conditions (see section 2). The corresponding elution diagrams are plotted in fig. 3. The partition coefficient $K_{av}$ of each fraction was computed according to eq. 2. The difference between the $K_{av}$ of two successive fractions was about 0.02. For this work, fractions having an elution volume close to that of the elution profile maximum were selected from the first set of chromatographic separations, and fractions with various elution volumes from the second chromatographic run of FD-20S.

### 3.2. Determination of the Stokes radius of dextran-FITC fractions

The FRAP curves of dextran-FITC fractions were measured with the laser beam in the vertical direction, as described in section 2. The temperature was between 20 and 22° C. There were only freely diffusing molecules ($L = 100\%$) in all experiments. The diffusion coefficients $D_0$ and Stokes radius were computed according to eqs. 3 and 5. An estimate of the molecular weight of each fraction was obtained from the following formula:

$$D_0 = 1.1 \times 10^{-4} \times M_w^{0.51} \tag{16}$$

This relation was established by Amu [33] who measured the diffusion coefficient of dextran fractions extracted from the bacterial strain NRRL

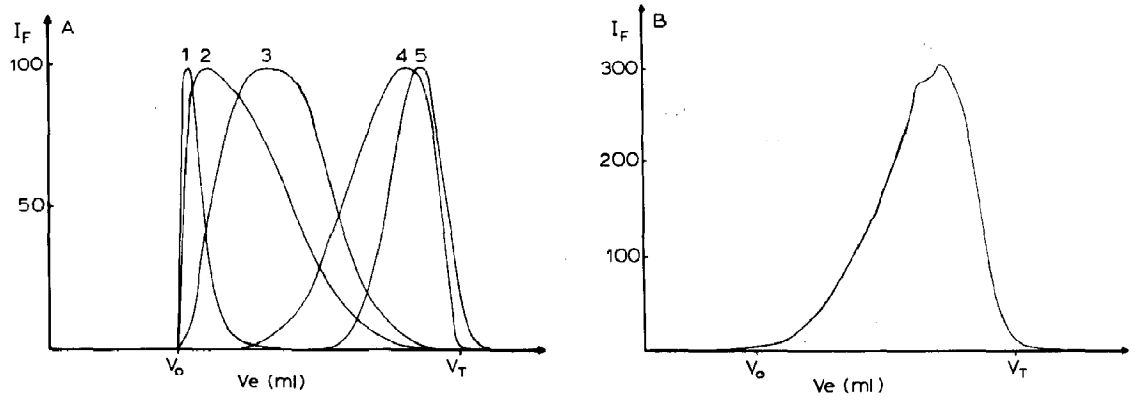


Fig. 3. Elution profiles of the six commercial lots of dextran-FITC chromatographed on Sephadex G-200. $I_F$, fluorescence intensity. (A) Chromatography of: 1, FD-150; 2, FD-70S; 3, FD-40S; 4, FD-10S; 5, FD-4. (B) Second chromatography of FD-20S.

Table 1

Characteristics of the dextran-FITC fractions studied in this work

Columns: (1) designation of commercial samples; (2) fraction number in chromatography on Sephadex G-200 column; (3) partition coefficient of fractions obtained from this column; (4) diffusion coefficient of the fraction in free aqueous solution (number of independent measurements in parentheses); (5) Stokes radius; (6) molecular weight of the fractions computed from eq. 16.

| (1) | (2) | (3) $K_{av}$ | (4) $D_0$ ($\mu m^2/s$) | | (5) $r_s$ (Å) | (6) $\bar{M}_w$ |
|---|---|---|---|---|---|---|
| FD-4 | 54 | 0.88 | 137±5 | (6) | 15.8±0.6 | 5400 |
| FD-20S (II) | 74 | 0.90 | 133±4 | (3) | 16 ± 0.6 | 5700 |
| FD-20S (II) | 69 | 0.82 | 109±3 | (3) | 19.7±0.6 | 8500 |
| FD-4 | 52 | 0.85 | 107±3 | (4) | 20 ± 0.5 | 8800 |
| FD-10S | 51 | 0.82 | 91±4 | (5) | 23 ± 1 | 12100 |
| FD-10S | 48 | 0.75 | 90±4 | (5) | 24 ± 0.9 | 12400 |
| FD-20S (II) | 64 | 0.73 | 89±4 | (3) | 24 ± 1 | 12800 |
| FD-10S | 49 | 0.77 | 85±3 | (4) | 25 ± 1 | 13800 |
| FD-20S (II) | 58 | 0.62 | 72± | 1(3) | 29.9±0.5 | 19300 |
| FD-20S (I) | 42 | 0.60 | 66±1 | (5) | 32.8±0.5 | 22700 |
| FD-20S (II) | 53 | 0.54 | 59±1 | (3) | 36.5±0.6 | 28500 |
| FD-20S (I) | 40 | 0.54 | 52±3 | (2) | 41 ± 2 | 36300 |
| FD-20S (II) | 47 | 0.43 | 44±1 | (3) | 48 ± 1 | 49500 |
| FD-40S | 35 | 0.43 | 43±1 | (5) | 49.9±1 | 51700 |
| FD-20S (II) | 42 | 0.35 | 58±2 | (3) | 57 ± 3 | 68400 |
| FD-70S | 30 | 0.31 | 37±3 | (4) | 58 ± 5 | 70700 |
| FD-40S | 29 | 0.28 | 33±2 | (3) | 65 ± 3.5 | 90400 |
| FD-20S (II) | 36 | 0.24 | 31±1 | (3) | 69 ± 2 | 100000 |
| FD-70S | 25 | 0.18 | 28±1 | (3) | 75 ± 3 | 119600 |
| FD-20S (II) | 31 | 0.14 | 28±1 | (3) | 77 ± 3 | 122900 |
| FD-150 | 22 | 0.10 | 22±2 | (5) | 98 ± 1 | 193800 |
| FD-150 | 21 | 0.08 | 21±0.5 | (4) | 101 ± 4 | 211400 |

B-512. The various parameters characterizing the FITC-dextran fractions are listed in table 1.

Our value of $D_0$ for the main fraction of the FD-150 sample was 22 $\mu m^2\ s^{-1}$ in agreement with the value determined by Peters [34], obtained for a nonfractionated FD-150 sample.

### *3.3. Microfluorimetric measurements of dextran-FITC permeation in Sephadex gel beads*

As shown in fig. 4, the microfluorimetric $K_{av}$ value, measuring the permeation of the dextran-FITC fractions in Sephadex G-200 gel beads, was found equal to the $K_{av}$ value computed from the volume at which the fraction eluted from the Sephadex G 200 column. This proves the validity of our microfluorimetric method. We found some variation of $K_{av}$ between the beads of the same gel lot, but there was no systematic relation between this variation and the bead diameter dispersion. In addition, we did not find any changes of $K_{av}$ at different spots inside a bead, which showed

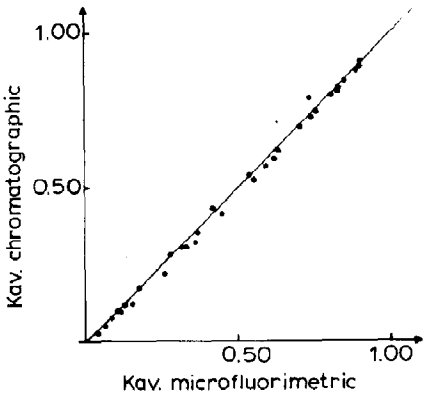


Fig. 4. Partition coefficient obtained from elution of dextran fractions on Sephadex G-200, as a function of the microfluorimetric partition coefficient of the fractions.

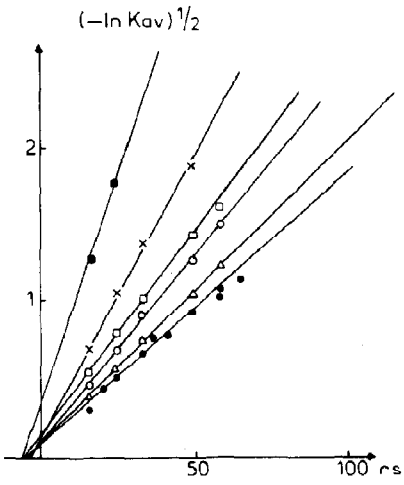


Fig. 5. Partition coefficient of dextran fractions as a function of Stokes radius of the molecules. G-200 (●), G-150 (△), G-100 (○), G-75 (□), G-50 (×), G-25 (■).

that the concentration distribution of dextran-FITC in a given bead was homogeneous.

### 3.4. *Variation in permeation of dextran-FITC in Sephadex gels with the Stokes radius of the solute*

We studied the partition coefficient $K_{av}$ of various dextran fractions, permeating in a given Sephadex gel, as a function of the Stokes radius $r_s$ of the dextran molecule. The points representing the experimental data in the coordinates $[(-\ln K_{av})^{1/2}, r_s]$ are situated on a straight line, as predicted by the formula of Laurent and Killander [14] (fig. 5). The parameters for this straight line were determined by linear regression, and the quantities $l$ and $r_f$ were computed from the slope and extrapolation of the straight lines according to eq. 11 while $\rho$ was obtained from eq. 12. The results of these calculations are given in table 2. According to eq. 10, $l$ should be proportional to the gel matrix concentration $C$. This held true for Sephadex G-200, G-150, G-100 and G-75 gels, as demonstrated in fig. 6. From the slope of this straight line, eq. 10 leads to $r_f = 10.7$ Å, larger than the average of the values reported in table 2. This difference might result from the nature of the gel model on which Ogston based his derivation of eq. 9. In this model, the gel network is assumed to

Table 2

Structural parameters of the Sephadex gels, obtained from application of eqs. 11 and 12, to measurements of the partition coefficients of dextran-FITC fractions

$l$, linear concentration of the Sephadex matrix; $r_f$, fiber cross-sectional radius; $\rho$, mean pore radius (eq. 12).

| Gel | $l$ (cm$^{-2}$) ($\times 10^{12}$) | $r_f$ (Å) | $\rho$ (Å) |
|---|---|---|---|
| G-200 | 0.87 | 7.80 | 50 |
| G-150 | 1.20 | 4.75 | 41 |
| G-100 | 1.80 | 4.20 | 33 |
| G-75 | 2.09 | 6 | 28.5 |
| G-50 | 3.98 | 4.3 | 21 |
| G-25 | 11 | 5.9 | 9 |

be formed by rigid fibers [13] while the Sephadex matrix is supposed to be constituted by flexible dextran molecules. This discrepancy might also arise from the nature of the solute molecules which are flexible chains and not rigid spheres as is assumed in the Ogston model.

### 3.5. *Diffusion of dextran-FITC fractions in Sephadex gel beads*

As described in section 2, these FRAP curves were obtained with the laser beams impinging on the sample in a direction perpendicular to the optical axis of the microscope. Two successive FRAP curves were plotted for each determination of $D/D_0$.

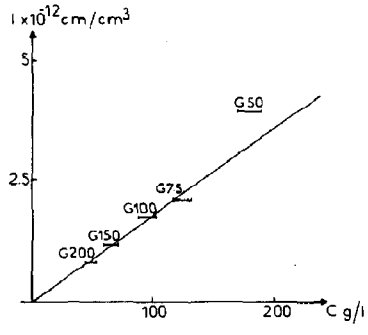


Fig. 6. Length concentration '$l$' as a function of the mass concentration of the Sephadex gel matrix. $l$ was computed from the slope of the lines in fig. 5.

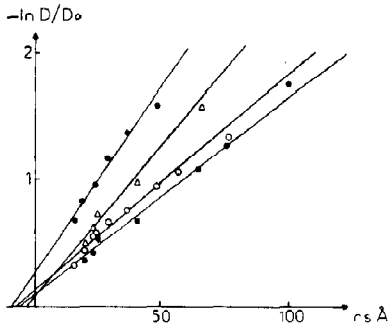


Fig. 7. Retardation ratio, $D/D_0$, of the diffusion of dextran-FITC fractions in the Sephadex gels, as a function of the Stokes radius of the dextran molecules. G-200 (●) (lower curve), G-150 (○), G-100 (△), G-75 (●) (upper curve).

These measurements were repeated five times for a given fraction and given gel bead. We also measured $K_{av}$ on the same bead.

### *3.6. Retardation of diffusion of dextran-FITC by Sephadex gel matrices as a function of the molecular solute Stokes radius*

The ratio $D/D_0$, which measures the retardation of dextran-FITC diffusion in a given Sephadex gel, was studied as a function of the molecular solute Stokes radius. The data obtained with Sephadex G-200, G-150, G-100 and G-75 are represented by the points for the coordinates $[-\ln D/D_0, r_s]$ in fig. 7. These points lie on a straight line as predicted by the theory of Ogston et al. [12]. The slope and intercepts of these lines were determined by linear regression analysis. We then obtained values of the cross-sectional radius and the linear concentration of fibers forming the gel matrix by applying eq. 14. These values are given in table 3. It can be seen that they are in fair agreement with the corresponding values obtained from the partitioning measurements (table 2).

Table 3

Structural parameters of the Sephadex gels, obtained from application of eqs. 12 and 14, to measurements of the diffusion retardation ratio $D/D_0$ of the dextran-FITC fractions

$l$, $r_f$ and $\rho$ have the same meaning as in table 2.

| Gel | $l$ (cm$^{-2}$) ($\times 10^{12}$) | $r_f$ (Å) | $\rho$ (Å) |
|---|---|---|---|
| G-200 | 0.77 | 4.5 | 52.5 |
| G-150 | 0.93 | 7.3 | 44.5 |
| G-100 | 1.83 | 2.75 | 34 |
| G-75 | 2.63 | 8.9 | 23.5 |

### *3.7. Relation between $D/D_0$ and $K_{av}$*

According to the theory of Ogston et al. [12], $K_{av}$ and $D/D_0$ are related by eq. 15. We investigated the validity of eq. 15 with $K_{av}$ and $D/D_0$ data measured on the same gel bead for various dextran-FITC fractions. The results obtained with Sephadex G-200, G-150 and G-100 (fig. 8A) verified well eq. 15. The agreement was not as good with Sephadex G-75, and even worse with G-50 (fig. 8B). For these two gels, the retardation of

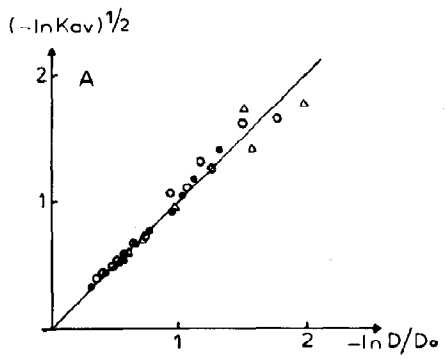


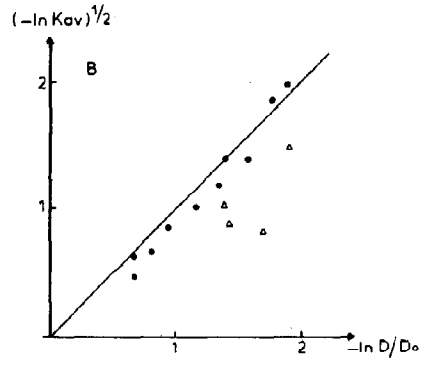


Fig. 8. Partition coefficient of the dextran-FITC fractions as a function of the retardation ratio in Sephadex gels. (A) Sephadex G-200 (○); G-150 (●); G-100 (△). (B) Sephadex G-75 (●); G-50 (△). $K_{av}$ and $D/D_0$ were measured on the same Sephadex bead.

molecular motion due to the gel matrix was greater than predicted by the theory, which might indicate some attractive interactions between the gel matrix and the solute molecules.

## 4. Discussion

In the present work, we determined the ratio $D/D_0$ of the diffusion coefficients of dextran molecules inside and outside Sephadex single gel beads, by measuring the fluorescence recovery after photobleaching in a part of the volume of a bead on the one hand, and in a small sample of equal volume of the free solution surrounding the bead on the other. The bleaching and monitoring beams pass through the sample cell perpendicularly to the optical axis of the microscope-photometer assembly which collects the fluorescence. The size of the volume which is defined by the laser beam diameter and the photometer measuring diaphragm was chosen to be much smaller than the size of the bead. With this optical configuration, the FRAP curve relative to the diffusion of molecules included in a bead was not perturbed by contributions from molecules situated in the surrounding solvent, a condition impossible to achieve with the usual episcopic illumination.

Working with a laser beam perpendicular to the microscope axis did not present difficulties, since the bead diameters were of the order of 100 $\mu$m. Therefore, the laser beam could be relatively wide and consequently not very convergent.

We felt it to be of interest to associate the measurements of $D/D_0$ with those of $K_{av}$, since both quantities are functions of the same structural parameters, namely the size of the solute molecules and the gel cavities. $K_{av}$ values were determined by a microfluorimetric method with the FRAP apparatus in which the excitation light was provided by the monitoring beam while the bleaching beam was permanently stopped.

We analysed our results on the permeation of dextran-FITC in a given gel by plotting $(-\ln K_{av})^{1/2}$ as a function of the Stokes radius of the dextran fractions. We found that the plot was linear according to expressions Ogston [13] and Laurent and Killander [14]. The slope of the straight line was proportional to the gel matrix concentration as predicted by the theory.

Ogston [13] assumed that the solute molecules were solid spheres. Dextrans have been extracted from the bacterium *Leuconostoc mesenteroides* NRRL B-512. The dextrans are polymers of glucose, 95% of which are linked by $(1 \rightarrow 6)$ bonds and form a flexible linear chain, while 5% are in side chains.

Chromatography based on permeation of polymer molecules in gels is sometimes influenced by side effects such as adsorption, partitioning or incompatibility [2]. However, when the eluant is a good solvent for the solute and the gel matrix, these effects are negligible. The partitioning coefficient $K_{av}$ is then equal to that of an equivalent solid sphere which has the same volume as the hydrodynamic of the solute molecule [2,35].

In the case of dextran, it has been shown that water is a good solvent [36–38]. Furthermore, Sephadex gels are mainly constituted of dextrans. These considerations may explain why the permeation of aqueous dextran solutions is rationalized by the formula of Laurent and Killander which is based on a model involving solid fibers and solid spheres. As noted above, the theoretical predictions of the model are not in complete agreement with our results, since the values computed from the slope of fig. 6 and extrapolation of the lines in fig. 5 are different. This discrepancy might arise from the difference between the structure of the gel and the solute molecules assumed in the model and the true nature of the Sephadex gel and of dextran molecules.

We measured the ratio of diffusion (retardation ratio) of dextran molecules inside and outside Sephadex gel beads. In the case of Sephadex G-200, G-150 and G-100, this retardation ratio decreased with increase in Stokes radius of the dextrans. In addition, $\ln(D/D_0)$ was found to be a linear function of $r_s$, in agreement with the theories of Ogston et al. [12] and Cukier [21]. Furthermore, the average fiber radius computed by applying eq. 14 to our diffusion measurements agreed with that determined by applying eq. 11 to our $K_{av}$ determination. Finally, eq. 15, which links the $K_{av}$ and $D/D_0$ values, was verified satisfactorily.

In future studies, it could be interesting to measure the values of $K_{av}$ and $D/D_0$ for other kinds of macromolecules and gels, and to ascertain the validity of these formulas in other experimental systems. A disagreement with these theoretical formulas might result from attractive interactions between the gel and solute macromolecules, or from the contribution of the reptation in the diffusion of flexible or elongated macromolecules [39].

Measurement of diffusion coefficients of macromolecular solutes in gels are interesting for several reasons:

(1) They allow a better evaluation of the factors influencing the efficiency of gel chromatography.

(2) They provide a means of studying interactions between a solute and a gel matrix.

(3) They can be considered as a model to help in interpreting macromolecular and vesicular motions in biological media such as the cytoplasm of living cells and in connective biological tissues [41].

## References


1 H. Determan, Gel chromatography (Springer-Verlag, New York, 1968).
2 K.H. Altgelt and J.C. Moore, in: Gel permeation chromatography in polymer fractionation, ed. Cantow (Academic Press, New York, 1967) ch. 84, p. 123.
3 L. Fisher, in: Laboratory techniques in biochemistry and molecular biology, eds. T.S. Work and E. Work (Elsevier, Amsterdam, 1969) vol 1, part II, p. 157.
4 J.C. Giddings, L.M. Bowman and M.N. Myers, Macromolecules 10 (1977) 443.
5 J.C. Giddings, Anal. Chem. 40 (1968) 2143.
6 G.K. Ackers and R.L. Steere, Biochim. Biophys. Acta 59 (1962) 137.
7 B.K. Davis, Proc. Natl. Acad. Sci. U.S.A. 71 (1974) 3120.
8 W. Mackie, D.B. Sellen and J. Sutcliffe, J. Polym. Sci. Polym. Symp. 61 (1977) 191.
9 T.C. Laurent and A. Pietruszkiewitz, Biochim. Biophys. Acta 49 (1961) 258.
10 T.C. Laurent, I. Bjork, A. Pietruszkiewitz and H. Persson, Biochim. Biophys. Acta 78 (1963) 351.
11 T.C. Laurent and H. Persson, Biochim. Biophys. Acta 83 (1964) 141.
12 A.G. Ogston, B.N. Preston and J.D. Wells, Proc. R. Soc. Lond. 333 (1973) 297.
13 A.G. Ogston, Trans. Faraday. Soc. 54 (1958) 1754.
14 T.C. Laurent and J. Killander, J. Chromatogr. 14 (1964) 317.
15 D. Langevin and F. Rondelez, Polymer 19 (1978) 875.
16 S.F. Edwards, Proc. Phys. Soc. Lond. 88 (1966) 265.
17 J. des Cloizeaux, J. Phys. (Paris) 36 (1975) 281.
18 P.G. de Gennes, P. Rincus, R.M. Velasco and F. Brochard, J. Phys. (Paris) 37 (1976) 1461.
19 A.M. Jamieson, J.G. Southwick and J. Blackwell, J. Polym. Sci. 20 (1982) 1513.
20 T.H. Lin and G.D.J. Phillies, J. Colloid Interface Sci. 100 (1984) 82.
21 R.I. Cukier, Macromolecules 17 (1984) 252.
22 K. Jacobson and J. Wojcieszyn, Proc. Natl. Acad. Sci. U.S.A. 81 (1984) 6747.
23 K. Luby-Phelps, D. Lansing Taylord and F. Lanni, J. Cell Biol. 102 (1986) 2015.
24 N.D. Gershon, K.R. Porter and B.L. Trus, Proc. Natl. Acad. Sci. U.S.A. 82 (1985) 5030.
25 Pharmacia Fine Chemicals, Gel filtration: theory and practice (Pharmacia, Uppsala, 1981).
26 P. Flodin, Dextran gels and their application in gel filtration Thesis (Pharmacia, Uppsala, 1962).
27 P. Wahl, Biophys. Chem. 22 (1985) 317.
28 T. Arvinte, K. Hildenbrand, P. Wahl and C. Nicolau, Proc. Natl. Acad. Sci. U.S.A. 83 (1986) 962.
29 D.E. Koppel, D. Axelrod, J. Schlessinger, E.L. Elson and W.W. Webb, Biophys. J. 16 (1976) 1315.
30 J. Yguerabide, J.A. Schmidt and E.E. Yguerabide, Biophys. J. 40 (1982) 69.
31 D. Axelrod, D.E. Koppel, J. Schlessinger, E.L. Elson and W.W. Webb, Biophys. J. 16 (1976) 1055.
32 C. Tanford, Physical chemistry of macromolecules (Wiley, New York, 1961).
33 T.C. Amu, Biophys. Chem. 16 (1982) 269.
34 R. Peters, EMBO J. 3 (1984) 1831.
35 H. Benoit, Z. Grubinic, P. Rempp, D. Decker and J. G. Zilliox, J. Chim. Phys. 63 (1966) 1507.
36 M. Wales, P.A. Marshall and S.G. Weissberg, J. Polym. Sci. 10 (1953) 229.
37 K.A. Granath, J. Colloid Sci. 13 (1958) 308.
38 A. Virnik, K. Khomyakov and I. Skokova, Russ. Chem. Rev. 44 (1975) 588.
39 P.G. De Gennes, J. Chem. Phys. 55 (1971) 572.
40 P.Y. Key and D.B. Sellen, J. Polym. Sci. Polym. Phys. 20 (1982) 659.
41 F.A. Meyer, M. Koblentz and A. Silberberg, Biochem J. 161 (1977) 285.